Recyclable Solid-Supported Catalysts for Quaternary Ammonium Iodide-Catalyzed Living Radical Polymerization

Chen-Gang Wang,[‡1] Jun Jie Chang,[‡1] Ellendea Yong Jing Foo,[1] Hiroshi Niino,[2] Shunsuke Chatani,[2] Shu Yao Hsu,[2] and Atsushi Goto[1]*

[1]Division of Chemistry and Biological Chemistry, School of Physical and Mathematical Sciences, Nanyang Technological University, 21 Nanyang Link, 637371 Singapore

[2]Hiroshima R&D Center, Mitsubishi Chemical Corporation, 20-1 Miyuki-cho, Otake, Hiroshima 739-0693, Japan

Abstract. Quaternary ammonium iodide ($R_4N^+I^-$) catalysts immobilized on silica particles, Fe_3O_4 magnetic particles, and organic resin particles were developed for organocatalyzed living radical polymerization. A random copolymer containing the catalytic $R_4N^+I^-$ moieties and the anchoring triethoxysilyl moieties was synthesized and immobilized onto silica and Fe_3O_4 particles to give the silica particle- and Fe_3O_4 particle-supported $R_4N^+I^-$ catalysts. A tertiary-amine-containing polymer resin particle was quaternized to give the resin particle-supported $R_4N^+I^-$ catalyst. The supported catalysts were successfully used to synthesize homopolymers and

block copolymers of methyl methacrylate, functional methacrylates, styrene, and acrylonitrile with low dispersities. The supported catalysts were able to be separated (recovered) from the polymerization solutions in simple manners, *i.e.*, with centrifugation or with a magnet. The catalysts were reused in five polymerization cycles without a noticeable decrease in the catalytic efficiency. The facile preparation of the supported catalysts, the broad monomer scope, and the feasibility of the catalyst reuse and recycle are attractive features.

INTRODUCTION

Covalently immobilized catalysts onto solid substrates have widely been used in synthetic chemistry.[1−4] Such immobilized (supported) heterogeneous catalysts are important in industries, because they facilitate catalyst removal and product purification compared with the corresponding homogeneous catalysts. The reuse and recycling of the supported catalysts offer waste-reducing, cost-saving, and "green" processes.[5,6]

In the field of polymerization, heterogeneous catalysts have been used for the commercial production of polyethylene and polypropylene using, *e.g.*, crystalline magnesium chloride-supported Ziegler-Natta catalysts since the 1970s.[7] To date, supported metallic catalysts for olefin polymerizations and metathesis polymerizations have extensively been studied.[8−11] Supported catalysts have also been utilized in living radical polymerization (LRP) (also known as reversible-deactivation radical polymerization). Transition-metal catalysts such as copper and ruthenium catalysts were immobilized onto silica,[12−16] crosslinked polymers,[12,13,17] clay,[18,19] magnetic particles,[20,21] and metal–organic frameworks[22,23] for atom transfer radical polymerization (ATRP). In reversible addition-fragmentation chain transfer (RAFT)

polymerization, silica- and fiber-supported organic photocatalysts were recently reported.[24–26] The use of supported catalysts has offered simplified polymer purification and prevention of catalyst residue contamination and coloration.[27,28]

Our research group has developed an organocatalyzed LRP using an alkyl iodide (R−I) as an initiator and an organic molecule as a catalyst.[29–34] The catalysts include amines, iodide anion (I^-), azide anion, and oxyanions. Mechanistically, polymer-iodide dormant species (polymer−I) coordinates a catalyst *via* a halogen bonding to form a complex (polymer−I···catalyst), which reversibly generates a propagating radical (polymer$^\bullet$) (Scheme 1a). This LRP was termed reversible complexation mediated polymerization (RCMP). RCMP is attractive because it does not require special capping agents or metal catalysts and is amenable to a wide range of monomers and polymer structures, including block copolymers, polymer brushes,[35,36] and micelles.[37,38]

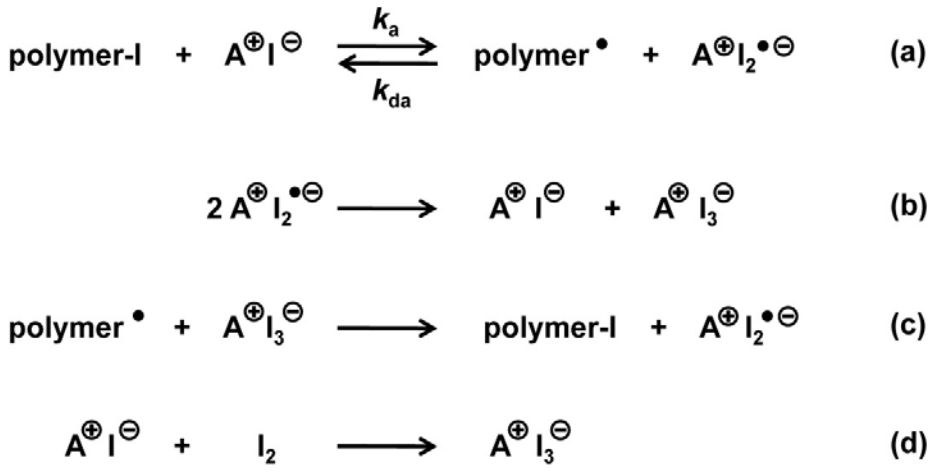

Scheme 1. (a) Reversible Activation and Deactivation, (b) Disproportionation of $A^+I_2^{\bullet-}$, (c) Deactivation with $A^+I_3^-$, and (d) Combination of A^+I^- and I_2 in RCMP.

In the present paper, we report the synthesis of supported RCMP catalysts and their use in the polymerizations. Quaternary ammonium iodide catalysts were immobilized onto silica nanoparticles, Fe_3O_4 magnetic nanoparticles, and crosslinked organic polystyrene resin particles. For the inorganic (silica and magnetic) particles, we designed and prepared a random copolymer containing catalytic quaternary ammonium iodide moieties and anchoring triethoxysilyl moieties (Scheme 2a). The polymer was subsequently immobilized on the particle surfaces through a silane coupling reaction between the triethoxysilyl groups and the hydroxyl groups on the inorganic oxide surfaces. For the organic resin particles, we used tertiary amine functionalized resin particles and quaternized the amine moieties to quaternary ammonium iodides (catalysts) (Scheme 2b). The obtained supported catalysts were used in the homopolymerizations and block copolymerizations of methyl methacrylate (MMA), functional methacrylates, styrene (St), and acrylonitrile (AN), yielding well-defined polymers. The catalysts were able to be separated (recovered) from the polymerization solutions by centrifugation or by applying a magnetic field. The reuse (recycling) of the recovered supported catalysts was attained multiple times without significant adverse effects to the catalytic activities. Figure 1 shows the studied alkyl iodide initiator and monomers. The low toxicity, inexpensiveness, ease of preparation, and reusability of the studied supported catalysts are attractive features.

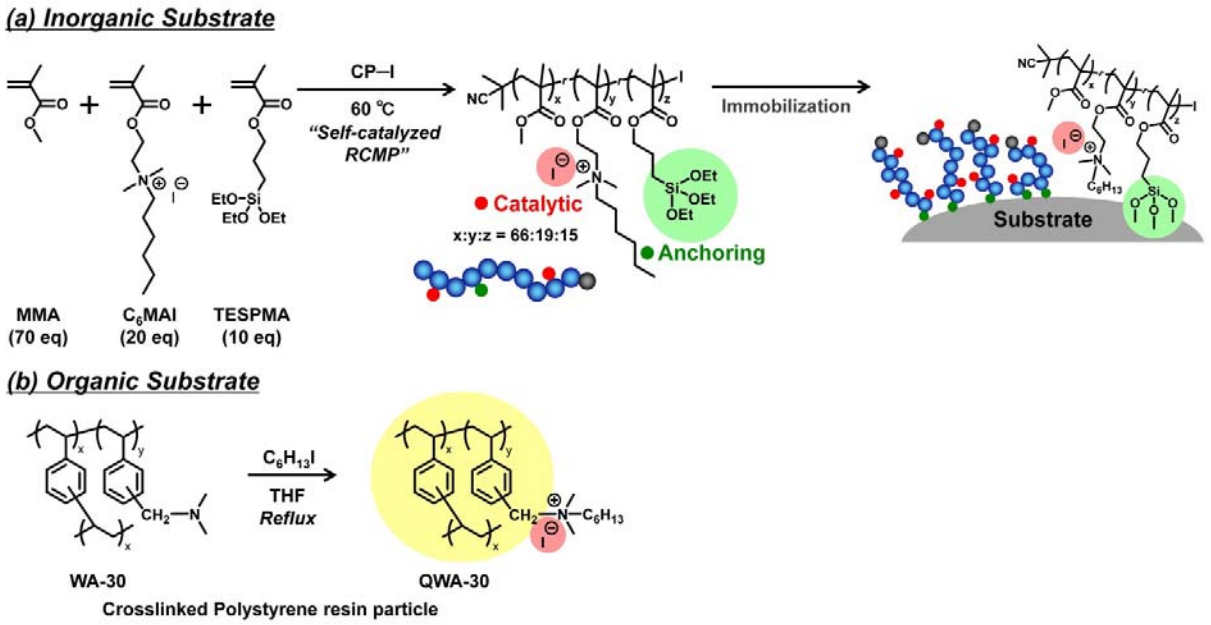

Scheme 2. Synthesis of Solid-supported Catalysts.

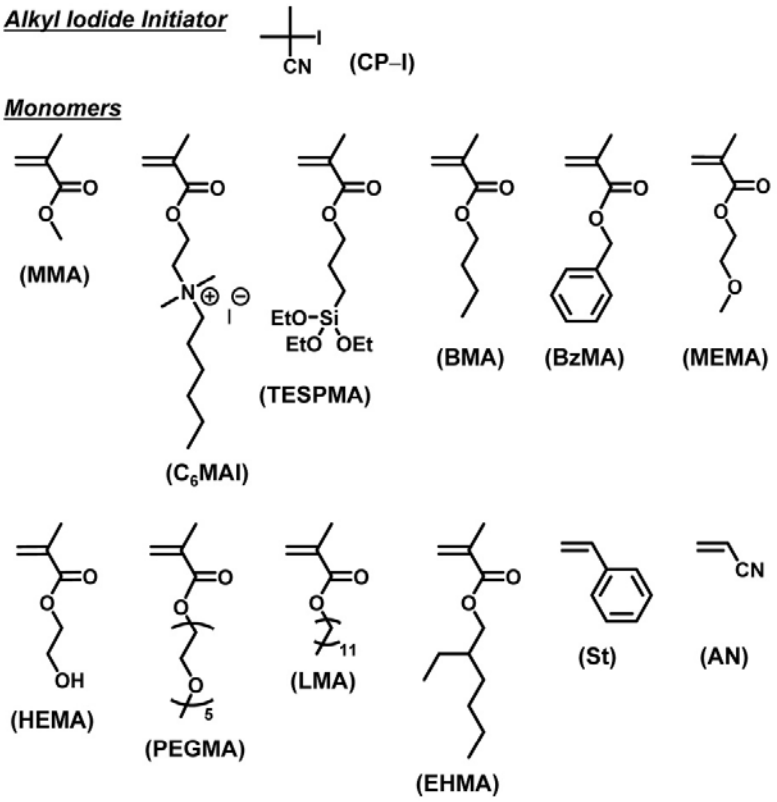

Figure 1. Structures of an alkyl iodide and monomers used in this work.

RESULTS AND DISCUSSION

Synthesis of Quaternary Ammonium Iodide-Containing Polymer and Preparation of Inorganic Particle-Supported Catalysts. A random copolymer with catalytic quaternary ammonium iodide moieties and anchoring triethoxysilyl moieties was synthesized *via* self-catalyzed RCMP (Scheme 2a).[39] We heated a mixture of MMA (70 equiv) as a spacing monomer, 2-(methacryloyloxy)ethyl]hexyl(dimethyl)ammonium iodide (C_6MAI, 20 equiv) as a catalytic monomer, 3-(triethoxysilyl)propyl methacrylate (TESPMA, 10 equiv) as an anchoring monomer, and 2-iodo-2-methylpropionitrile (CP−I (Figure 1), 1 equiv) as an alkyl iodide dormant initiator at 60 °C. The polymerization was stopped at 3 h (total monomer conversion = 67%), giving a PMMA-*r*-PC_6MAI-*r*-PTESPMA random copolymer (M_n = 7000 and $Đ = M_w/M_n$ = 1.21) after purification, where PMMA, PC_6MAI, and PTESPMA are the polymers of MMA, C_6MAI, and TESPMA, respectively, M_n and M_w are the number- and weight-average molecular weights, respectively, and $Đ$ is the dispersity. The average MMA/C_6MAI/TESPMA molar ratio in the copolymer after purification was determined to be 66/19/15 from the ^{1}H NMR peak areas of the copolymer (Figure S1 in Supporting Information). The PMMA-*r*-PC_6MAI-*r*-PTESPMA was immobilized onto silica (average diameter = 12 nm) and Fe_3O_4 (diameter = 50–100 nm) particles through a silane coupling reaction between the triethoxysilyl groups in the TESPMA units and the hydroxyl groups on the particle surfaces, yielding the corresponding supported catalysts (Scheme 2a).

Preparation of Organic Particle-Supported Catalysts. We used DIAION WA-30 (produced by Mitsubishi Chemical) (Scheme 2b), which is a commercially available organic crosslinked polystyrene particle (diameter = 300–900 μm) containing tertiary amino groups. The particles were reacted with 1-iodohexane to quaternize the tertiary amino groups *via* the Menshutkin

reaction, yielding quaternary ammonium iodide functionalized WA-30 particles (QWA-30) (Scheme 2b). The amount of the quaternary ammonium iodide was calculated to be 2.5 mmol per gram of the obtained QWA-30 from the consumption of 1-iodohexane. The extent of the quaternization would have a gradient from the outermost surface to the inner core of the particle. X-ray photoelectron spectroscopy (XPS) showed that at least the outer most surface (a few nanometers thick) of the particle was almost fully (~90%) quaternized (as described below) and would work as a catalytic interface.

Surface Characterization. Figures 2a and 2b show the XPS spectra of the original and quaternary ammonium iodide-immobilized silica particles, respectively. Two peaks at 618 and 628 eV for iodide 3d electrons were observed in Figure 2b, demonstrating the successful immobilization of the quaternary ammonium iodide. The thermal gravimetric analysis (TGA) of the immobilized particles (Figure 3) showed a 5% weight-loss at 350 °C and an 11% weight-loss at 460 °C. The first 5% weight loss is attributed to the decomposition of the side chains of the C_6MAI and TESPMA units. The 11% weight-loss is attributed to the complete decomposition of the polymer. From the weight loss, the content of the quaternary ammonium iodide was calculated to be 0.12 mmol per gram of the immobilized silica particles (Supporting information). The successful immobilization of the quaternary ammonium iodide was also confirmed for the magnetic particles (0.05 mmol per gram of the immobilized magnetic particle) (Figures S3 and S4 in Supporting Information).

For the organic particle, Figures 2c and 2d show the XPS spectra of the original WA-30 and quaternized QWA-30 particles. After the quaternization (Figure 2d), the iodide 3d electrons (618 and 628 eV) newly appeared and the nitrogen 1s electron signal shifted from 399 eV (uncharged

nitrogen atom (Figure 2c)) to 402 eV (positively charged nitrogen atom N^+ (Figure 2d)),[40] confirming the preparation of the quaternized QWA-30 particles.

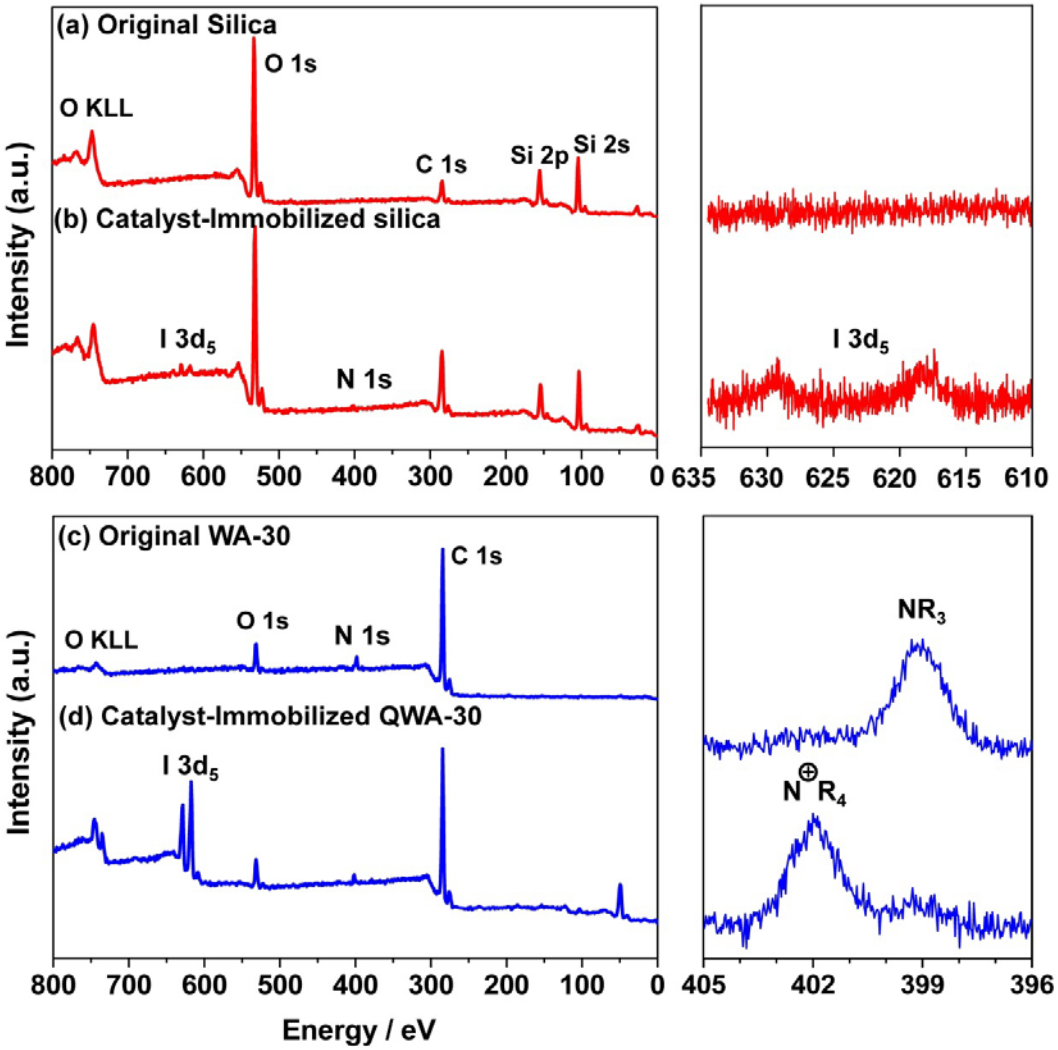

Figure 2. XPS spectra of (a) original silica, (b) catalyst-immobilized silica, (c) WA-30, and (d) QWA-30.

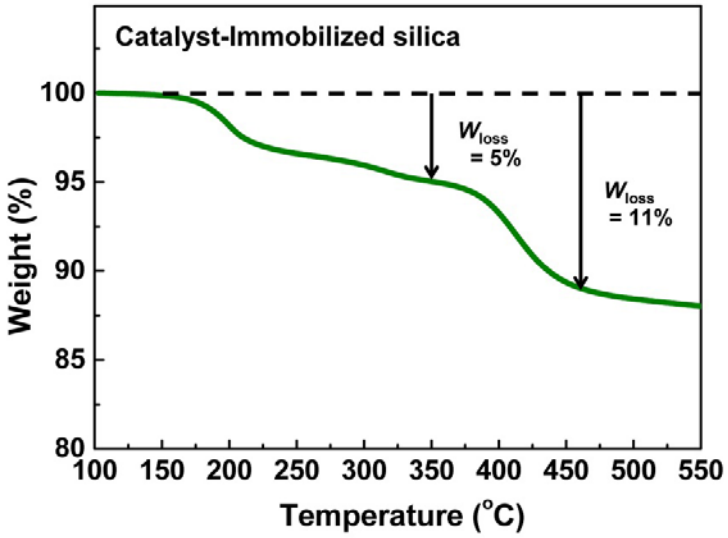

Figure 3. TGA curve of quaternary ammonium iodide-immobilized silica (at the heating rate of 10 °C/min under N_2 (flow rate = 100 mL/min)). W_{loss} denotes the weight loss.

Polymerizations of MMA. The supported catalysts were used in the polymerizations of MMA. Because the catalysts are present only on the particle surfaces (heterogeneous system), the overall concentrations of the catalysts (activator and deactivator) in the solution may need to be adjusted differently from those in the corresponding homogeneous system. As in ATRP, the activation of the dormant species to generate polymer$^{\bullet}$ is usually a chemically controlled process, and its overall rate would not largely be affected by the heterogeneous local concentration of the activator. Therefore, we may use a similar overall concentration of the activator to that in the homogeneous system. In contrast, the deactivation of polymer$^{\bullet}$ with a deactivator to generate the dormant species is nearly a diffusion controlled process, and its overall rate would largely be affected by the heterogeneity in the local concentration of the deactivator.[41] Therefore, we would need to use a much higher overall concentration of the deactivator than that in the homogeneous system so that polymer$^{\bullet}$ can sufficiently rapidly react with the deactivator. The required overall

concentration of the deactivator is a key difference between the homogeneous and supported catalyst systems.

A deactivator in the present system is $A^+I_2^{\bullet-}$ (Scheme 1a). Two unstable $A^+I_2^{\bullet-}$ radicals can undergo disproportionation into A^+I^- (mono-iodide) and $A^+I_3^-$ (tri-iodide) (Scheme 1b).[30] $A^+I_3^-$ is another deactivator (Scheme 1c). The concentration of the $A^+I_3^-$ deactivator can be increased by the addition of I_2 in the system through a reaction of the activator A^+I^- and I_2 for generating $A^+I_3^-$ (Scheme 1d). Therefore, in the present study, we optimized the deactivator concentration with the addition of I_2, as described below.

Table 1. Bulk Polymerizations of MMA with R-I, catalyst and I_2.

Entry	Supported Catalyst	$[MMA]_0/[CP–I]_0/[I_2]_0/[AIBN]_0$ (mM)[a]	T (°C)	t (h)	Conv (%)[b]	M_n[c] ($M_{n,theo}$[d])	$Đ$[c]
1	Silica (10wt%, 10 mM)	8000/80/0/0	70	24	53	6300 (5300)	1.43
2	Silica (10wt%, 10 mM)	8000/80/2/0	70	24	38	4500 (3800)	1.24
3	Silica (10wt%, 10 mM)	8000/80/10/120	70	4	85	7600 (8500)	1.22
4	Silica (5wt%, 5 mM)	8000/80/10/120	70	4	91	8300 (9100)	1.31
5	Silica (2wt%, 2 mM)	8000/80/10/120	70	4	61	6900 (6100)	1.61
6	Fe_3O_4 (25wt%, 10 mM)	8000/80/10/120	70	4	90	7300 (9000)	1.25
7	QWA-30 (1wt%, 20 mM)	8000/80/8.4/80	70	4	95	8900 (9500)	1.24
C1	None	8000/80/0/0	70	24	No polymerization		
C2	Homogeneous catalyst BNI (10 mM)	8000/80/0/0	70	12	73	7300 (7800)	1.18
C3	Original silica (10wt%)[e]	8000/80/10/120	70	4	81	7400 (8100)	1.58
C4	None	8000/80/0/120	70	4	99	9000 (9900)	1.72
C5	None[f]	8000/80/10/120	70	4	98	6600 (9800)	1.81
C6	WA-30 (1wt%, 20 mM)	8000/80/8.4/80	70	4	87	8900 (8700)	1.21

[a]The addition of 25wt% toluene (MMA/toluene = 3/1 (w/w)) for entries 1-6 and C1-C5 and 20wt% toluene (MMA/toluene = 4/1 (w/w)) for entries 7 and C6. [b]The monomer conversions determined from the GPC peak areas of polymers. [c]PMMA-calibrated THF-GPC values. [d]Theoretical M_n calculated with $[MMA]_0$, $[CP–I]_0$ and monomer conversion. [e]Original silica without iodide immobilization. [f]A solution of MMA and the silica-supported catalyst was heated at 50 °C with stirring for 2 h. After removing the silica-supported catalyst from the MMA solution, the MMA solution was mixed with CP−I (80 mM), I_2 (10 mM), and AIBN (120 mM) and heated at 70 °C.

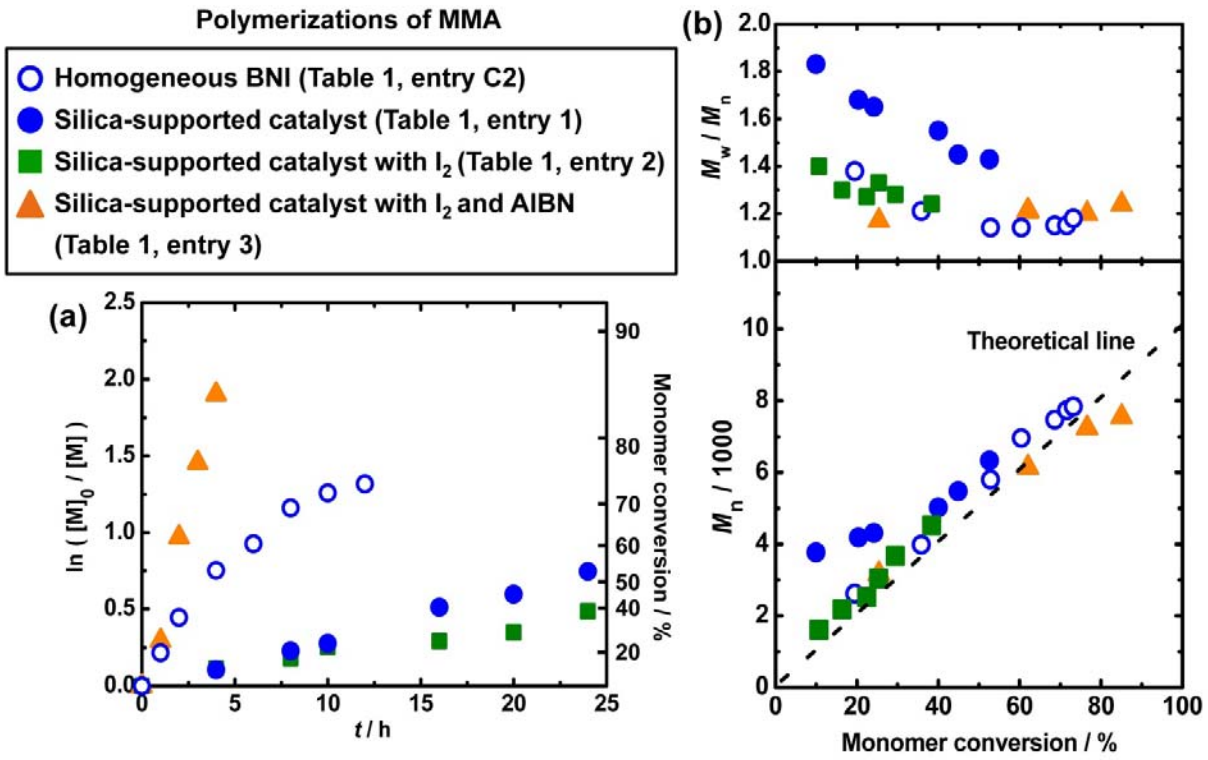

Figure 4. Plots of (a) $\ln([M]_0/[M])$ vs t and (b) M_n and M_w/M_n vs monomer conversion for the MMA/CP−I/I_2/AIBN/catalyst systems (70 °C). The reaction conditions are given in Table 1. The symbols are indicated in the figure.

Table 1 (entries 1−5) and Figure 4 summarize the polymerization results of MMA with silica-supported catalysts. The solvent was toluene (25% toluene and 75% MMA). A solution of toluene, MMA (100 eq), CP−I (1 eq), and silica-supported catalyst (0.12 eq, 10wt% of MMA) was heated at 70 °C in the absence and presence of I_2 (0 or 0.025 eq) as a deactivator. In the absence of I_2 (Table 1 (entry 1) and Figure 4 (filled circle)), the polymerization reached a 53% monomer conversion after 24 h. No polymerization took place without the addition of the silica-supported catalyst (Table 1, entry C1), meaning that the polymerization was induced by the

silica-supported catalyst. At an early stage of polymerization (Figure 4 (filled circle)), the M_n value was larger than the theoretical M_n ($M_{n,theo}$) value calculated from [MMA], [CP−I], and the monomer conversion, and the $Đ$ value was relatively large (>1.5). This result suggests insufficient amounts of the deactivators ($A^+I_2^{\bullet-}$ and $A^+I_3^-$) present in the early stage of polymerization, causing the addition of many monomers to polymer$^\bullet$.

For comparison, Table 1 (entry C2) and Figure 4 (open circle) show the polymerization with a homogeneous catalyst tetrabutylammonium iodide (BNI) at the same activator concentration. BNI gave a 73% monomer conversion after 12 h, leading to a faster polymerization than the silica-supported catalyst (Table 1 (entry 1) and Figure 4 (filled circle)). The M_n value agreed with the $M_{n,theo}$ value, and the $Đ$ value was relatively small (1.2−1.4) from an early stage of polymerization, suggesting that the BNI system had a sufficiently high deactivation rate. Small amounts of the deactivators ($A^+I_2^{\bullet-}$ and $A^+I_3^-$) were generated in situ in the polymerization by the so-called persistent radical effect,[42,43] and this amount was large enough to give the sufficiently high deactivation rate in the homogeneous BNI system.

In the heterogeneous system, larger overall amounts of the deactivators were required, as mentioned above. The addition of I_2 (Table 1 (entry 2) and Figure 4 (square)) successfully led to a good agreement of the M_n values with the $M_{n,theo}$ values and low $Đ$ values (= 1.24−1.40) from an early stage of polymerization, suggesting that polymer$^\bullet$ was deactivated sufficiently rapidly. The amount of the added I_2 (20% to the activator (= 2 mM/10 mM)) was relatively large for the mentioned reason. After 24 h, the monomer conversion reached 38%, yielding a PMMA with a low $Đ$ value of 1.24.

Despite the good control in the M_n and $Đ$ values, the polymerization was relatively slow (38% monomer conversion for 24 h) (Table 1 (entry 2) and Figure 4 (square)). The slow polymerization was overcome by the addition of an azo initiator, *i.e.*, 2,2'-azobis(isobutyronitrile) (AIBN, 120 mM) (Table 1 (entry 3) and Figure 4 (triangle)). Azo initiators are often used to effectively increase the polymerization rate in other living radical polymerizations.[43] We also added a larger amount of I_2 (10 mM) to secure the sufficiently fast deactivation. The polymerization rate increased by a factor of 8, reaching an 85% monomer conversion for 4 h with keeping a relatively low $Đ$ value of 1.22. We were also able to reduce the amount of the supported catalyst from 10wt% to 5wt% at a similar level of polymerization control, attaining a 91% monomer conversion in 4 h with a $Đ$ value of 1.31 (Table 1 (entry 4)). A further reduction in the catalyst amount to 2wt% resulted in a high $Đ$ value of 1.61 (Table 1 (entry 5)).

With the addition of AIBN, the low $Đ$ values (1.22−1.31) were attained only in the presence of the supported catalyst. (The role of AIBN was to increase the polymerization rate but not decrease the $Đ$ value.) For comparison, the use of the original silica (without catalyst) resulted in a large $Đ$ value of 1.58 (Table 1 (entry C3)). Without the catalyst, the system (containing only MMA, CP−I and AIBN) is iodide transfer polymerization (ITP).[44] Because of the relatively low frequency of the degenerative chain transfer of iodide, the $Đ$ value was 1.72 (Table 1 (entry C4)).

To confirm that the iodide catalyst was strongly immobilized on the silica surface during the polymerization, a solution of MMA and the silica-supported catalyst was heated at 50 °C with stirring for 2 h. After removing the supported catalyst from the MMA solution, the MMA solution was mixed with CP−I (80 mM), AIBN (120 mM), and I_2 (10 mM) and heated at 70 °C.

This comparison system (Table 1 (entry C5)) resulted in a large $Đ$ value of 1.81, demonstrating that the iodide catalyst strongly bonded on the silica surface and did not bleed into the MMA solution. This result also importantly suggests that the supported catalyst may be reused in a recycled manner (as demonstrated below).

The Fe_3O_4 magnetic particle-supported catalyst was also effective in the polymerization of MMA (Table 1 (entry 6)). Because the magnetic particle was covered with a smaller amount of the catalyst (0.05 mmol per gram of the particle) than the silica particle (0.12 mmol per gram of the particle), we loaded a large amount (25wt%) of the magnetic particle, yielding a polymer with M_n of 7300 and $Đ$ of 1.25 for 4 h (monomer conversion = 90%). Importantly, the magnetic particle-supported catalyst was able to be separated from the polymerization solution by simply using a magnet (Figure 5). The magnetic separation is a time-saving process and is attractive for the ease of catalyst separation and recycling.

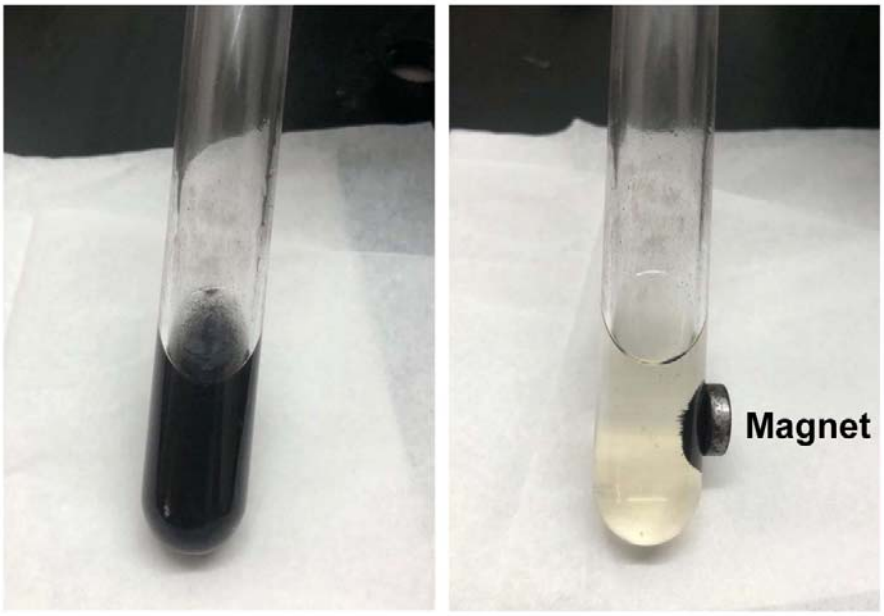

Figure 5. Separation of Fe_3O_4-supported catalyst from the PMMA solution with a magnet.

Besides the inorganic particles, organic particle-supported catalyst QWA-30 was also effective (Table 1 (entry 7) and Figure 6 (square)). The 1wt% of QWA-30 in MMA (20 mM of catalyst) yielded a polymer with M_n = 8900 and $Đ$ = 1.24 for 4 h (monomer conversion = 95%). QWA-30 is a porous particle (Figure S6 in Supporting Information) carrying a high concentration of quaternary ammonium iodide (2.5 mmol per gram of the particle), which is 20 times higher than that of the silica particle (0.12 mmol per gram of the particle). Tertiary amines were reported to work as moderately efficient RCMP catalysts.[29] The unquaternized (tertiary amine containing) WA-30 was also able to be used as a catalyst for the polymerization under the same reaction condition, giving PMMA with M_n = 8900 and $Đ$ = 1.21 (Table 1 (entry C6) and Figure 6 (triangle)). The polymerization rate with the unquaternized WA-30 catalysts was slightly lower than that with the quaternized QWA-30 (Figure 6).

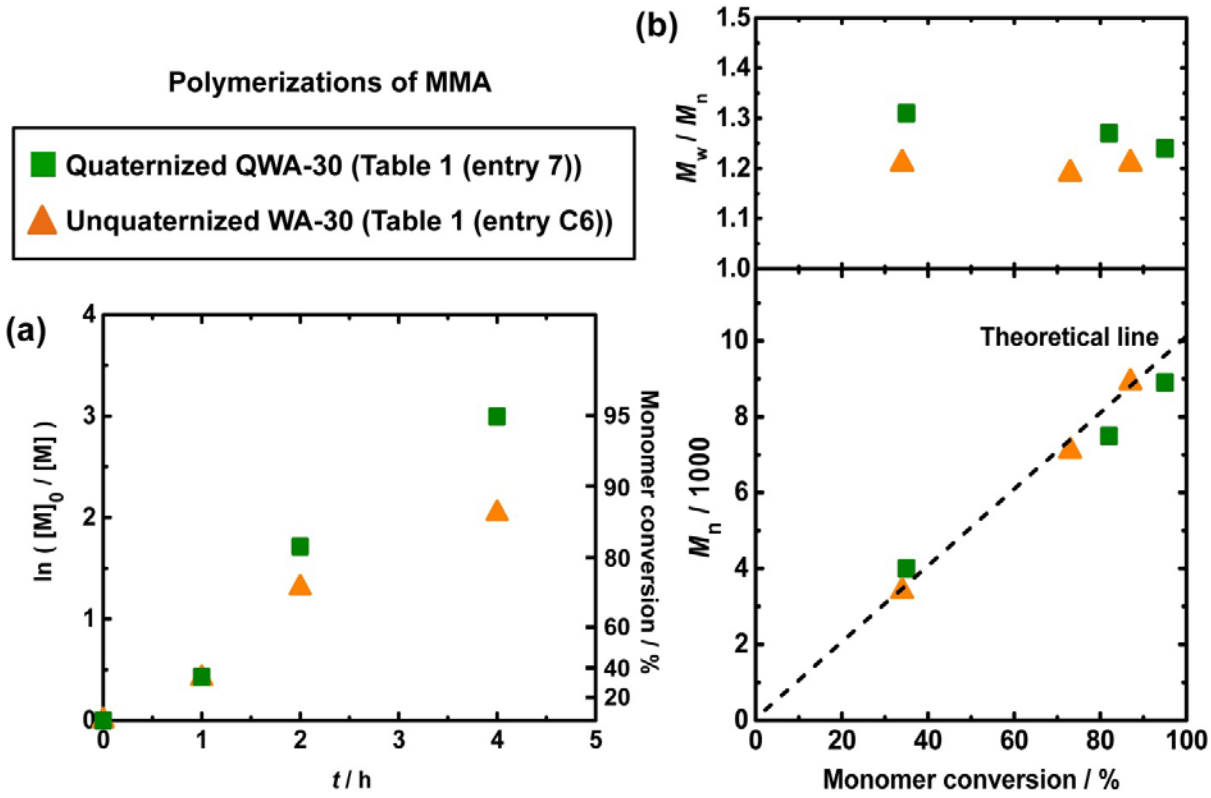

Figure 6. Plots of (a) ln([M]$_0$/[M]) vs t and (b) M_n and M_w/M_n vs monomer conversion for the MMA/CP−I/I$_2$/AIBN/catalyst systems (70 °C). The reaction conditions are given in Table 1. The symbols are indicated in the figure.

Polymerizations with Recycled Catalysts. The supported catalysts were able to be separated (recovered) from the polymerization solutions through centrifugation (silica and organic resin particles) or with magnet (magnetic particles) in simple and effective manners. Also, iodide anions (catalysts) are firmly associated with the quaternary ammonium cations immobilized on the particles because of the electronic neutralization. Therefore, the recovered support catalysts do not significantly lose their catalytic activities. In order to demonstrate the recyclability, we used the recovered silica-supported catalyst and resin-supported catalyst

(QWA-30) in the polymerizations of MMA under the same reaction conditions (Table 1 (entries 3 and 7), respectively) in recycled manners. Using the silica-supported catalyst, the monomer conversion (85%−95%), M_n value (7700−9200), and $Đ$ value (1.23−1.35) were consistently sustained in the five polymerization cycles (Figure 7a and Table S1 in Supporting Information). The high conversions and low $Đ$ values demonstrate the high recyclability. We added I_2 in each run, because I_2 was washed out from the particle in the recovery process.

For the resin-supported QWA-30 catalyst (Figure 7b and Table S2 in Supporting Information), I_2 was added only in the first polymerization cycle, and no additional I_2 was added in the second and subsequent cycles. The resin particle was porous, and I_2 seemed to be adsorbed in the pores. Visually (Figure 7c), the quaternized QWA-30 was colorless before the polymerization because of no color of I^- and became brown after the first polymerization run because of the addition of I_2 to generate brown I_3^-. The brown color did not significantly become lighter in the subsequent runs, qualitatively suggesting insignificant loss of I_3^- (or I_2). As Figure 7b shows, the monomer conversion (88%−95%), M_n value (8900−9600), and $Đ$ value (1.20−1.31) were consistently sustained in the five runs, demonstrating the good recyclability. The recyclability is attractive for the reduction in the chemical waste.

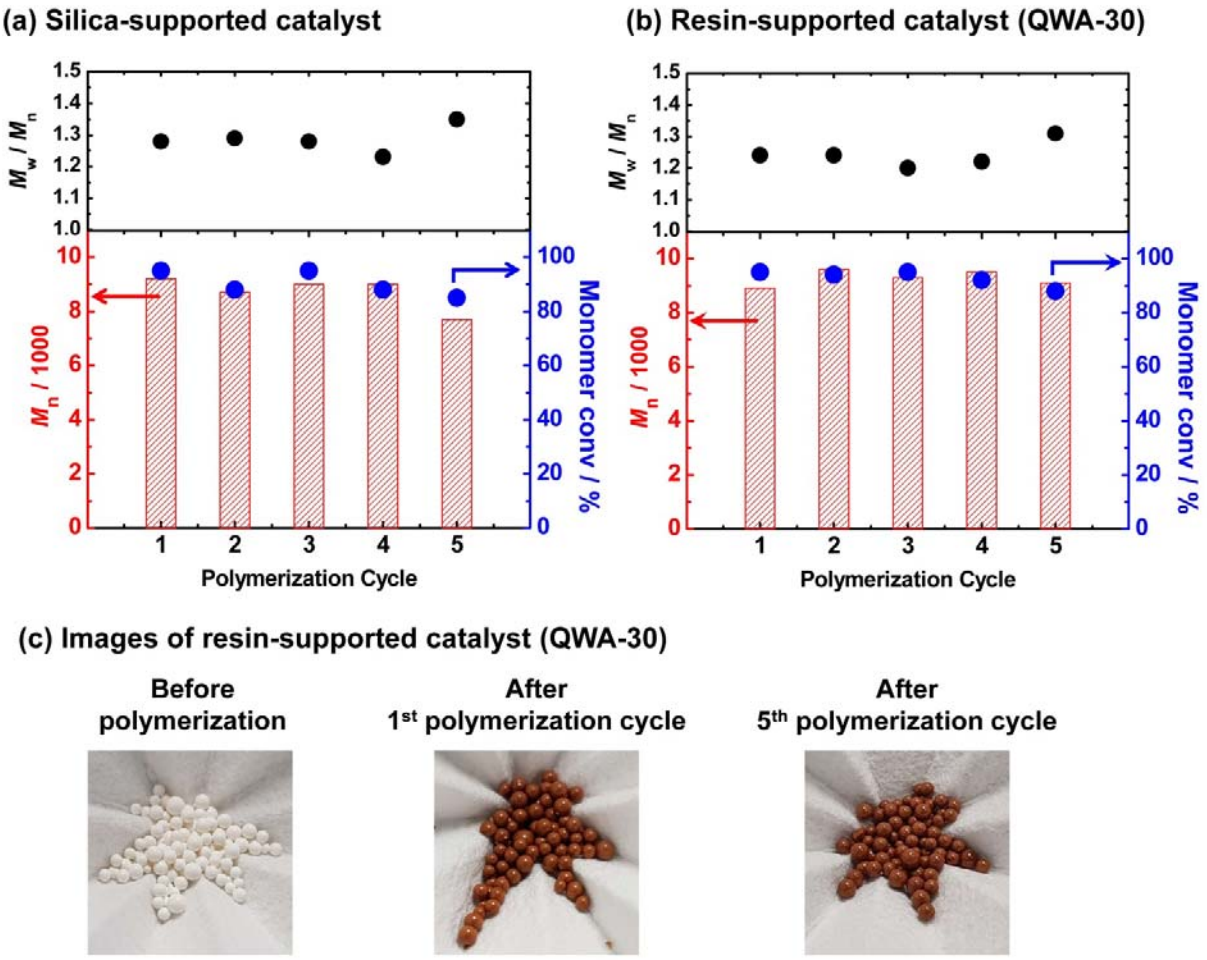

Figure 7. Polymerizations of MMA with the recycled use of (a) silica-supported catalyst and (b) resin-supported catalyst QWA-30. The reaction conditions are given in entries 3 and 7 in Table 1, respectively. (c) Images of resin-supported catalyst QWA-30 before polymerization, after the first polymerization cycle, and after the fifth polymerization cycle.

Polymerizations of Functional Methacrylates, Styrene and Acrylonitrile. The silica- and resin-supported catalysts were amenable to several functional methacrylates (Figure 1), styrene (St), and acrylonitrile (AN) (Table 2). The polymerizations were successful for butyl methacrylate (BMA (entry 1)), benzyl methacrylate (BzMA (entry 2)), 2-methoxyethyl

methacrylate (MEMA (entry 3)), 2-hydroxyethyl methacrylate (HEMA (entry 4)), poly(ethylene glycol) methyl ether methacrylate (PEGMA (entry 5)), lauryl methacrylate (LMA (entry 8)), and 2-ethylhexyl methacrylate (EHMA (entry 9)) as functional methacrylates, and St (entry 6) and AN (entry 7) as other families of monomer, attaining the $Đ$ values of 1.22−1.42 at monomer conversions of 64%–98% for 2–8 h. For the hydrophilic HEMA and PEGMA, the temperature was lowered to 50 °C with the addition of 2,2'-azobis(2,4-dimethylvaleronitrile) (V65) as an azo initiator in order to suppress the HI elimination from the polymer chain end. The HI elimination is enhanced in polar solutions. These results demonstrate the large monomer scope of the studied supported catalysts.

Table 2. Polymerizations of Methacrylates, St, and AN.

Entry	Supported Catalyst	Monomer	Azo initiator	Solvent[a]	$[Monomer]_0/[CP-I]_0/[I_2]_0$ /[Azo initiator]$_0$ (mM)	T (°C)	t (h)	Conv (%)[b]	M_n[c] ($M_{n,theo}$[d])	$Đ$[c]
1	Silica (10wt%, 14 mM)	BMA	AIBN	Toluene	8000/80/10/120	70	4	92	14000 (16000)	1.39
2	Silica (10wt%, 17 mM)	BzMA	AIBN	Toluene	8000/80/10/120	70	4	67	12000 (9700)	1.28
3	Silica (10wt%, 14 mM)	MEMA	AIBN	Toluene	8000/80/10/120	70	4	74	9100 (10000)	1.22
4	Silica (10wt%, 12 mM)	HEMA	V65	None	8000/80/10/120	50	8	66	14000 (20000)	1.24
5	Silica (10wt%, 29 mM)	PEGMA	V65	None	8000/80/5/80	50	2	64	9100 (10000)	1.34
6	Silica (10wt%, 10 mM)	St	AIBN	Toluene	8000/80/10/80	80	6	84	7200 (8700)	1.40
7	Silica (10wt%, 5 mM)	AN	AIBN	EC[e]	8000/80/5/40	75	4	92	12000 (4900)	1.42
8	QWA-30 (1wt%, 51 mM)	LMA	AIBN	Toluene	8000/80/21.6/160	70	4	96	18000 (24000)	1.26
9	QWA-30 (1wt%, 40 mM)	EHMA	AIBN	Toluene	8000/80/16.8/200	70	4	98	12000 (19000)	1.23

[a]The addition of 25wt% solvent (monomer/solvent = 3/1 (w/w)) for entries 1−3, 6, and 7 and 40wt% solvent to monomer (monomer/toluene = 6/4 (w/w)) for entries 8 and 9. [b]Monomer conversions determined from the ^{1}H NMR peak areas of remaining monomers. [c]PMMA-calibrated THF-GPC values for entries 1−3, 6, 8 and 9. PMMA-calibrated DMF-GPC values for entries 4, 5, and 7. [d]Theoretical M_n calculated with $[Monomer]_0$, $[R-I]_0$, and monomer conversion. [e]Ethylene carbonate.

Block Polymerizations. The supported catalysts also afforded block copolymers (Table 3 and Figure 8). The silica- and resin-supported catalysts were used to prepare PMMA-iodide (PMMA−I) macroinitiators (with M_n = 4200 and $Đ$ = 1.24 and with M_n = 4500 and $Đ$ = 1.26,

respectively, after the reprecipitation) (Supporting Information). The supported catalysts were separated (recovered) from the polymerization solutions by centrifugation and reused in the block polymerizations. Using the PMMA−I macroinitiators and the recycled catalysts, block polymerization of several monomers, *i.e.,* BzMA, St, PEGMA, and LMA, yielded low-dispersity block copolymers with M_n = 8500−17000 and $Đ \leq 1.45$ (Table 3). A large fraction of the PMMA−I macroinitiators extended to block copolymers (Figure 8), demonstrating the high block-efficiency. The results show an accessibility to various block copolymers, including hydrophobic-hydrophobic, hydrophobic-hydrophilic, and hard-soft block copolymers.

Table 3. Block polymerizations with PMMA−I macroinitiators and recycled catalysts.

Entry	Supported Catalyst	Monomer	Azo	Solvent[a]	$[Monomer]_0/[PMMA{-}I^b]_0/[I_2]_0/[Azo]_0$ (mM)	T (°C)	t (h)	Conv (%)[c]	M_n[d] ($M_{n,theo}$[e])	$Đ$[d]
1	Silica (10wt%, 17 mM)	BzMA	AIBN	Toluene	8000/80/10/120	70	3	97	16000 (21000)	1.20
2	Silica (10wt%, 10 mM)	St	AIBN	Toluene	8000/80/10/80	80	4	80	8500 (12000)	1.45
3	Silica (10wt%, 29 mM)	PEGMA	V65	None	8000/80/5/80	50	2	49	16000 (19000)	1.21
4	QWA-30 (1wt%, 51 mM)	LMA	AIBN	Diglyme	8000/80/0/160	70	4	82	17000 (25000)	1.45

[a]The addition of 25wt% toluene (25wt% of toluene and 75wt% of monomer and PMMA−I) for entries 1 and 2 and 36wt% diglyme (36wt% of diglyme and 64wt% of monomer and PMMA−I) for entry 4. [b]PMMA−I (M_n = 4200 and $Đ$ = 1.24) for entries 1−3 and PMMA−I (M_n = 4500 and $Đ$ = 1.26) for entry 4. [b]Monomer conversions determined from the ^{1}H NMR peak areas of the remaining monomers. [d]PMMA-calibrated THF-GPC values for entries 1, 2 and 4. PMMA-calibrated DMF-GPC value for entry 3. [e]Theoretical M_n calculated with $[Monomer]_0$, $[PMMA{-}I]_0$, and monomer conversion.

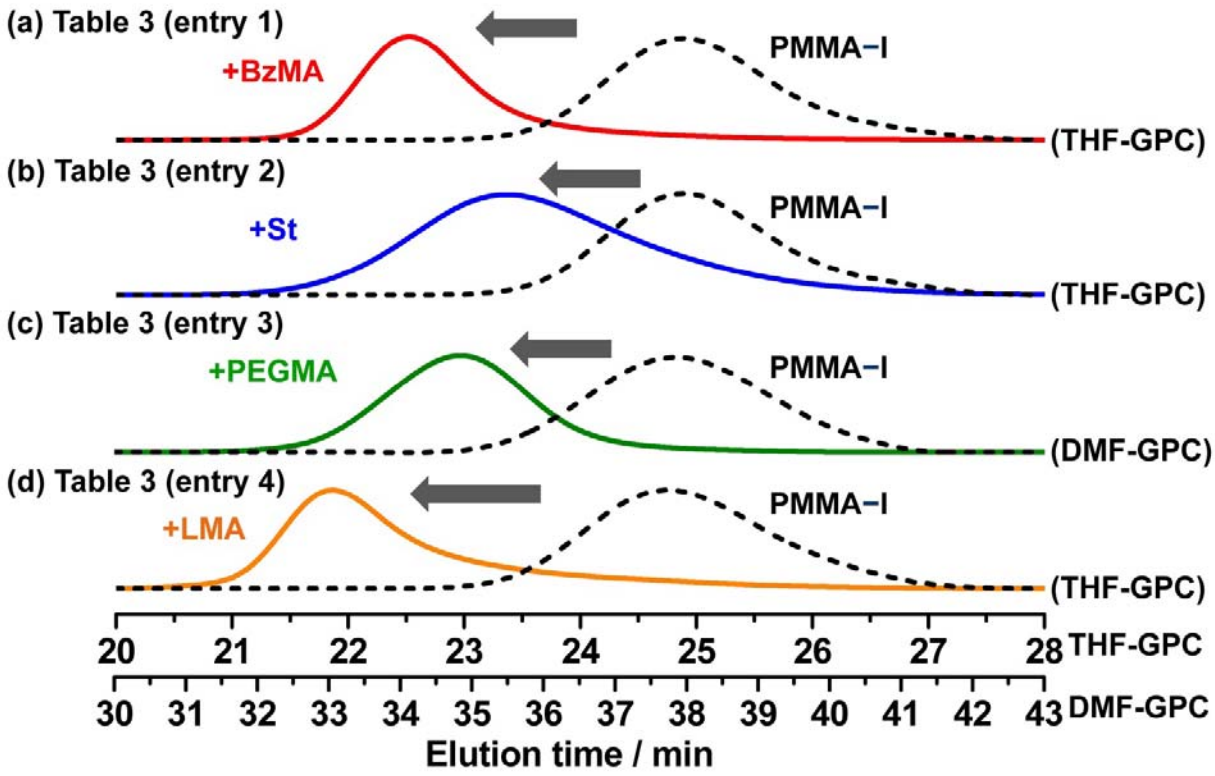

Figure 8. GPC chromatograms before (dashed lines) and after (solid lines) the block polymerizations (Table 3).

CONCLUSIONS

Silica particle-, magnetic particle-, and organic resin particle-supported catalysts were developed for RCMP. The supported catalysts afforded well-defined homopolymers and block copolymers of MMA, functional methacrylates, St, and AN with small $Đ$ values. The supported catalysts were separated from the polymerization solution in simple manners (with centrifugation or with a magnet) and re-used in further polymerizations in recycled manners. The facile preparation of the supported catalysts, the broad monomer scope, and the feasibility of the catalyst reuse and recycle are attractive features.

ASSOCIATED CONTENT

Supporting Information. The Supporting Information is available free of charge on the ACS Publications website at http://pubs.acs.org.

Materials, measurement, experimental procedures, ^{1}H NMR spectra of PMMA-*r*-PC_6MAI-*r*-PTESPMA and PMMA−I, thermogravimetric analysis of silica- and Fe_3O_4-supported catalysts, SEM images of supported catalysts, experimental data for recycled use of supported catalysts in the polymerizations of MMA.

AUTHOR INFORMATION

Corresponding Author

*E-mail: agoto@ntu.edu.sg

Author Contributions

‡These authors contributed equally. (C.-G. Wang and J. J. Chang)

ORCID

C.-G Wang: 0000-0001-6986-3961

A. Goto: 0000-0001-7643-3169

Notes

The authors declare no competing financial interest.

ACKNOWLEDGMENT

This work was supported by National Research Foundation (NRF) Investigatorship in Singapore (NRF-NRFI05-2019-0001) and Academic Research Fund (AcRF) Tier 2 from Ministry of Education in Singapore (MOE2017-T2-1-018). E. Y. J. Foo acknowledges The URECA undergraduate research programme.

REFERENCES

(1) McNamara, C. A.; Dixon, M. J.; Bradley, M. Recoverable Catalysts and Reagents Using Recyclable Polystyrene-Based Supports. *Chem. Rev.* **2002**, *102*, 3275−3300.

(2) Corma, A.; Garcia, H. Silica-Bound Homogenous Catalysts as Recoverable and Reusable Catalysts in Organic Synthesis. *Adv. Synth. Catal.* **2006**, *348*, 1391−1412.

(3) Gawande, M. B.; Branco, P. S.; Varma, R. S. Nano-magnetite (Fe_3O_4) as a Support for Recyclable Catalysts in the Development of Sustainable Methodologies. *Chem. Soc. Rev.* **2013**, *42*, 3371−3393.

(4) Copéret, C.; Allouche, F.; Chan, K. W.; Conley, M. P.; Delley, M. F.; Fedorov, A.; Moroz, I. B.; Mougel, V.; Pucino, M.; Searles, K.; Yamamoto, K.; Zhizhko, P. A. Bridging the Gap between Industrial and Well-Defined Supported Catalysts. *Angew. Chem. Int. Ed.* **2018**, *57*, 6398−6440.

(5) Fechete, I.; Wang, Y.; Vedrine, J. C. The past, present and future of heterogeneous catalysis. *Catal. Today.* **2012**, *189*, 2−27.

(6) Schlögl, R. Heterogeneous Catalysis. *Angew. Chem. Int. Ed.* **2015**, *54*, 3465−3520.

(7) Böhm, L. L. The Ethylene Polymerization with Ziegler Catalysts: Fifty Years after the Discovery. *Angew. Chem. Int. Ed.* **2003**, *42*, 5010−5030.

(8) Heurtefeu, B.; Bouilhac, C.; Cloutet, E.; Taton, D.; Deffieux, A.; Cramail, H. Polymer Support of "Single-site" Catalysts for Heterogeneous Olefin Polymerization. *Prog. Polym. Sci.* **2011**, *36*, 89−126.

(9) Klapper, M.; Joe, D.; Nietzel, S.; Krumpfer, J. W.; Müllen, K. Olefin Polymerization with Supported Catalysts as an Exercise in Nanotechnology. *Chem. Mater.* **2014**, *26*, 802−819.

(10) Hübner, S.; de Vries, J. G.; Farina, V. Why Does Industry Not Use Immobilized Transition Metal Complexes as Catalysts? *Adv. Synth. Catal.* **2016**, *358*, 3−25.

(11) Stürzel, M.; Mihan, S.; Mülhaupt, R. From Multisite Polymerization Catalysis to Sustainable Materials and All-Polyolefin Composites. *Chem. Rev.* **2016**, *116*, 1398−1433.

(12) Kickelbick, G.; Paik, H.-j.; Matyjaszewski, K. Immobilization of the Copper Catalyst in Atom Transfer Radical Polymerization. *Macromolecules* **1999**, *32*, 2941−2947.

(13) Haddleton, D. M.; Duncalf, D. J.; Kukulj, D.; Radigue, A. P. 3-Aminopropyl Silica Supported Living Radical Polymerization of Methyl Methacrylate: Dichlorotris(triphenylphosphine)ruthenium(II) Mediated Atom Transfer Polymerization. *Macromolecules* **1999**, *32*, 4769−4775.

(14) Shen, Y.; Zhu, S.; Zeng, F.; Pelton, R. H. Atom Transfer Radical Polymerization of Methyl Methacrylate by Silica Gel Supported Copper Bromide/Multidentate Amine. *Macromolecules* **2000**, *33*, 5427−5431.

(15) Nguyen, J. V.; Jones, C. W. Design, Behavior, and Recycling of Silica-Supported CuBr-Bipyridine ATRP Catalysts. *Macromolecules* **2004**, *37*, 1190−1203.

(16) Bernhardt, C. Osman, C. B.; Charleux, B.; Stoffelbach, F. New Supported-catalytic Systems for Atom Transfer Radical Polymerization. *Polymer* **2015**, **77**, 199−207.

(17) Taskin, O. S.; Kiskan, B.; Yagci, Y. An Efficient, Heterogeneous, Reusable Atom Transfer Radical Polymerization Catalyst. *Polym. Int.* **2018**, *67*, 55−60.

(18) Munirasu, S.; Aggarwal, R.; Baskaran, D. Highly Efficient Recyclable Hydrated-clay Supported Catalytic System for Atom Transfer Radical Polymerization. *Chem. Commun.* **2009**, 45, 4518−4520.

(19) Barrientos-Ramírez, S.; Montes de Oca-Ramírez, G.; Ramos-Fernández, E. V.; Sepúlveda-Escribano, A.; Pastor-Blas, M. M.; González-Montiel, A. Surface Modification of Natural Halloysite Clay Nanotubes with Aminosilanes. Application as Catalyst Supports in the Atom Transfer Radical Polymerization of Methyl Methacrylate. *Appl. Catal., A.* **2011**, *406*, 22−33.

(20) Ding, S.; Xing, Y.; Radosz, M.; Shen, Y. Magnetic Nanoparticle Supported Catalyst for Atom Transfer Radical Polymerization. *Macromolecules* **2006**, *39*, 6399−6405.

(21) Kanazawa, A.; Satoh, K.; Kamigaito, M. Iron Oxides as Heterogeneous Catalysts for Controlled/Living Radical Polymerization of Styrene and Methyl Methacrylate. *Macromolecules* **2011**, *44*, 1927−1933.

(22) Lee, H.-C.; Antonietti, M.; Schmidt, B. V. K. J. A Cu(II) Metal–Organic Framework as a Recyclable Catalyst for ARGET ATRP. *Polym. Chem.* **2016**, *7*, 7199−7203.

(23) Lee, H.-C.; Fantin, M.; Antonietti, M.; Matyjaszewski, K.; Schmidt, B. V. K. J. Synergic Effect between Nucleophilic Monomers and Cu(II) Metal−Organic Framework for Visible-Light-Triggered Controlled Photopolymerization. *Chem. Mater.* **2017**, *29*, 9445−9455.

(24) Shanmugam, S.; Xu, S.; Adnan, N. N. M.; Boyer, C. Heterogeneous Photocatalysis as a Means for Improving Recyclability of Organocatalyst in "Living" Radical Polymerization. *Macromolecules* **2018**, *51*, 779−790.

(25) Huang, Y.; Li, X.; Li, J. L.; Zhang, B.; Cai, T. An Environmentally Benign and pH-Sensitive Photocatalyst with Surface-Bound Metalloporphyrin for Heterogeneous Catalysis of Controlled Radical Polymerization. *Macromolecules* **2018**, *51*, 7974−7982.

(26) Chu, Y.; Corrigan, N.; Wu, C.; Boyer, C.; Xu, J. A Process for Well-Defined Polymer Synthesis through Textile Dyeing Inspired Catalyst Immobilization. *ACS Sustainable Chem. Eng.* **2018**, *6*, 15245−15253.

(27) Tsarevsky, N. V.; Matyjaszewski, K. "Green" Atom Transfer Radical Polymerization: From Process Design to Preparation of Well-Defined Environmentally Friendly Polymeric Materials. *Chem. Rev.* **2007**, *107*, 2270−2299.

(28) Ding, M.; Jiang, X.; Zhang, L.; Cheng, Z.; Zhu, X. Recent Progress on Transition Metal Catalyst Separation and Recycling in ATRP. *Macromol. Rapid Commun.* **2015**, *36*, 1702−1721.

(29) Goto, A.; Suzuki, T.; Ohfuji, H.; Tanishima, M.; Fukuda, T.; Tsujii, Y.; Kaji, H. Reversible Complexation Mediated Living Radical Polymerization (RCMP) Using Organic Catalysts. *Macromolecules* **2011**, *44*, 8709−8715.

(30) Goto, A.; Ohtsuki, A.; Ohfuji, H.; Tanishima, M.; Kaji, H. Reversible Generation of a Carbon-centered Radical from Alkyl Iodide Using Organic Salts and their Application as Organic Catalysts in Living Radical Polymerization. *J. Am. Chem. Soc.* **2013**, *135*, 11131−11139.

(31) Wang, C.-G.; Goto, A. Solvent-Selective Reactions of Alkyl Iodide with Sodium Azide for Radical Generation and Azide Substitution and Their Application to One-Pot Synthesis of Chain-End-Functionalized Polymers. *J. Am. Chem. Soc.* **2017**, *139*, 10551−10560.

(32) Wang, C.-G.; Hanindita, F.; Goto, A. Biocompatible Choline Iodide Catalysts for Green Living Radical Polymerization of Functional Polymers. *ACS Macro Lett.* **2018**, *7*, 263−268.

(33) Liu, X.; Wang, C.-G.; Goto, A. Polymer Dispersity Control by Organocatalyzed Living Radical Polymerization. *Angew. Chem. Int. Ed.* **2019**, *58*, 5598−5603.

(34) Xu, H.; Wang, C.-G.; Lu, Y.; Goto, A. Pyridine *N*-Oxide Catalyzed Living Radical Polymerization of Methacrylates *via* Halogen Bonding Catalysis. *Macromolecules* **2019**, *52*, 2156−2163.

(35) Wang, C.-G.; Chen, C.; Sakakibara, K.; Tsujii, Y.; Goto, A. Facile Fabrication of Concentrated Polymer Brushes with Complex Patterning by Photocontrolled Organocatalyzed Living Radical Polymerization. *Angew. Chem. Int. Ed.* **2018**, *57*, 13504−13508.

(36) Wang, C.-G.; Yong, H. W.; Goto, A. Effective Synthesis of Patterned Polymer Brushes with Tailored Multiple Graft Densities. *ACS Applied Materials & Interfaces* **2019**, *11*, 14478−14484.

(37) Zheng, J.; Wang, C.-G.; Yamaguchi, Y.; Miyamoto, M.; Goto, A. Temperature-Selective Dual Radical Generation from Alkyl Diiodide: Applications to Synthesis of Asymmetric CABC

Multi-block Copolymers and Their Unique Assembly Structures. *Angew. Chem. Int. Ed.* **2018**, *130*, 1568−1572.

(38) Sarkar, J.; Xiao, L.; Jackson, A. W.; van Herk, A. M.; Goto, A. Synthesis of Transition-metal-free and Sulfur-free Nanoparticles and Nanocapsules *via* Reversible Complexation Mediated Polymerization (RCMP) and Polymerization Induced Self-assembly (PISA). *Polym. Chem.* **2018**, *9*, 4900−4907.

(39) Wang, C.-G.; Oh, X. Y.; Liu, X.; Goto, A. Self-Catalyzed Living Radical Polymerization Using Quaternary-Ammonium-Iodide-Containing Monomers. *Macromolecules* **2019**, *52*, 2712−2718.

(40) Yao, C.; Li, X.; Neoh, K.-G.; Shi, Z.; Kang, E.-T. Surface Modification and Antibacterial Activity of Electrospun Polyurethane Fibrous Membranes with Quaternary Ammonium Moieties. *J. Membrane Sci.* **2008**, *320*, 259−267.

(41) Hong, S. C.; Matyjaszewski, K. Fundamentals of Supported Catalysts for Atom Transfer Radical Polymerization (ATRP) and Application of an Immobilized/Soluble Hybrid Catalyst System to ATRP. *Macromolecules* **2002**, *35*, 7592−7605.

(42) Fischer H. The persistent radical effect: A principle for selective radical reactions and living radical polymerizations. *Chem. Rev.* **2001**, *101*, 3581−3610.

(43) Goto, A.; Fukuda, T. Kinetics of Living Radical Polymerization. *Prog. Polym. Sci.* **2004**, *29*, 329−385.

(44) David, G.; Boyer, C.; Tonnar, J.; Ameduri, B.; Lacroix-Desmazes, P.; Boutevin, B. Use of Iodocompounds in Radical Polymerization. *Chem. Rev.* **2006**, *106*, 3936−3962.

For Table of Contents use only